ACS APPLIED MATERIALS & INTERFACES

Research Article

www.acsami.org

Rational Design of Aggregation-Induced Emission Luminogen with Weak Electron Donor−Acceptor Interaction to Achieve Highly Efficient Undoped Bilayer OLEDs

Long Chen,[†] Yibin Jiang,[‡] Han Nie,[†] Rongrong Hu,[†] Hoi Sing Kwok,[‡] Fei Huang,[†] Anjun Qin,[†] Zujin Zhao,*[,†] and Ben Zhong Tang*[,†,§]

[†]Guangdong Innovative Research Team, SCUT−HKUST Joint Research Laboratory, State Key Laboratory of Luminescent Materials and Devices, South China University of Technology (SCUT), Guangzhou 510640, China

[‡]Center for Display Research, The Hong Kong University of Science & Technology (HKUST), Clear Water Bay, Kowloon, Hong Kong, China

[§]Department of Chemistry, Institute for Advanced Study, Institute of Molecular Functional Materials, Division of Life Science, Division of Biomedical Engineering and State Key Laboratory of Molecular Neuroscience, HKUST, Clear Water Bay, Kowloon, Hong Kong, China

Supporting Information

ABSTRACT: In this work, two tailored luminogens (TPE-NB and TPE-PNPB) consisting of tetraphenylethene (TPE), diphenylamino, and dimesitylboryl as a π-conjugated linkage, electron donor, and electron acceptor, respectively, are synthesized and characterized. Their thermal stabilities, photophysical properties, solvachromism, fluorescence decays, electronic structures, electrochemical behaviors, and electroluminescence (EL) properties are investigated systematically, and the impacts of electron donor−acceptor (D−A) interaction on optoelectronic properties are discussed. Due to the presence of a TPE unit, both luminogens show aggregation-induced emission, but strong D−A interaction causes a decrease in emission efficiency and red-shifts in photoluminescence and EL emissions. The luminogen, TPE-PNPB, with a weak D−A interaction fluoresces strongly in solid film with a high fluorescence quantum yield of 94%. The trilayer OLED [ITO/NPB (60 nm)/TPE-PNPB (20 nm)/TPBi (40 nm)/LiF (1 nm)/Al (100 nm)] utilizing TPE-PNPB as a light emitter shows a peak luminance of 49 993 cd m^{-2} and high EL efficiencies up to 15.7 cd A^{-1}, 12.9 lm W^{-1}, and 5.12%. The bilayer OLED [ITO/TPE-PNPB (80 nm)/TPBi (40 nm)/LiF (1 nm)/Al (100 nm)] adopting TPE-PNPB as a light emitter and hole transporter simultaneously affords even better EL efficiencies of 16.2 cd A^{-1}, 14.4 lm W^{-1}, and 5.35% in ambient air, revealing that TPE-PNPB is an eximious p-type light emitter.

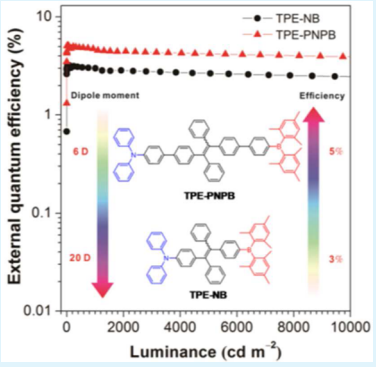

KEYWORDS: *aggregation-induced emission, tetraphenylethene, electron donor−acceptor, hole transporter, organic light-emitting diodes*

INTRODUCTION

In recent decades, considerable efforts have been made toward the development of organic luminescent materials that fulfill a series of items such as efficient light emission,[1,2] balanced charges,[3,4] high thermal stability,[5,6] etc. for the sake of fabricating high-performance organic light-emitting diodes (OLEDs). Among these factors, high photoluminescence (PL) efficiency is the essential one for a light emitter. However, most luminescent materials built with conventional π-conjugated planar chromophores suffer from the notorious concentration- or aggregation-caused quenching (ACQ). Their good light emissions in solutions are weakened greatly when fabricated into solid films, which depresses the device performances, presenting a thorny obstacle to the evolution of OLEDs. The doping method may alleviate the ACQ problem, but it requires hard-to-control techniques and may cause other adverse effects, such as phase separation and unstable emission colors at high voltages.[7−9] In 2001, Tang et al.[10−14] found that certain propeller-like luminogens that were almost nonfluorescent in solutions became highly emissive as the aggregate formation. Such a novel phenomenon coined as aggregation-induced emission (AIE) challenges the ACQ effect. The combination of AIE-active units and conventional ACQ building blocks has generated various luminogens with excellent solid-state emission, which function outstandingly as light-emitting layers for undoped OLEDs, demonstrating a promising avenue to solve the ACQ problem of luminescent materials.[15−23]

To achieve high-performance OLEDs, the balance of holes and electrons in a device is another crucial issue to be addressed

Received: July 31, 2014
Accepted: September 11, 2014
Published: September 11, 2014

dx.doi.org/10.1021/am505036a | ACS Appl. Mater. Interfaces 2014, 6, 17215−17225

successfully. The bipolar luminescent materials are favored to facilitate the injection and transport of holes and electrons and, thus, to improve the exciton recombination efficiency. The introduction of bipolar emitters is also anticipated to reduce the active layers, which is helpful in simplifying the device configuration and cutting down on manufacture cost as well. Since the charge-carrier transport in small molecules is a chain of redox processes between the neutral molecules and the corresponding radical ions, electron-donating and -withdrawing moieties have the potential ability to transport holes and electrons, respectively.[24] Therefore, the most widely adopted protocol to build bipolar materials is to incorporate electron donor−acceptor (D−A) combinations into the same molecule.[25−27] In addition, through proper selection of D−A substituents, the energy levels of the luminogens can be finely modulated, which makes it highly possible to achieve a breakthrough in electroluminescence (EL) efficiencies via a thermally activated delay fluorescence[28,29] or a hybridized local and charge-transfer excited state (HLCT).[30]

With these considerations, integrating of AIE merit within a D−A framework is envisioned as an effective approach to create solid-state emissive bipolar materials. To achieve a synergistic effect, the D−A interaction should be regulated carefully and deliberately, for it governs the PL and EL properties of the generated luminogens greatly. The clues to structure−property relationship are thus meaningful for a new system combining AIE effect and D−A interaction. Herein, two tailored luminogens with different D−A intereaction strengths are designed and synthesized, where tetraphenylethene (TPE) is adopted as an AIE-active bridge and diphenylamino and dimesitylboryl serve as an electron donor and acceptor, respectively. The reasons for the molecular design principle are as follows. TPE is an intriguing AIE luminogen with a simple molecular structure and is emerging as a favorable building block to construct solid-state emitters for OLEDs.[15−23,31,32] On the other hand, diphenylamino is a good electron-rich group and is widely used to construct hole-transporting materials, while dimesitylboryl is an electron-deficient one, due to the vacant low-lying p_π orbital on the boron center, which is conducive to improving the electron-transporting ability of the molecule.[33−36] The results show that both luminogens possess AIE characteristics and are highly fluorescent in solid films with high PL efficiencies up to 94%. They can function as efficient p-type light emitters in OLEDs, and the undoped bilayer devices based on them afford excellent EL efficiencies of 16.2 cd A^{-1}, 14.4 lm W^{-1}, and 5.35%. Furthermore, the significant impacts of D−A interaction on the PL and EL properties of the molecules are investigated and elucidated, which deserves judicious consideration in the design of multifunctional light emitters in the future.

EXPERIMENTAL SECTION

Materials and Instruments. THF was distilled from sodium benzophenone ketyl under dry nitrogen immediately prior to use. All other chemicals and reagents were purchased from Aldrich and J&K Scientific Ltd. and used as received without further purification. ^{1}H and ^{13}C NMR spectra were measured on a Bruker AV 400 spectrometer or Bruker AV 600 spectrometer in appropriated deuterated solution at room temperature. High resolution mass spectra (HRMS) were recorded on a GCT premier CAB048 mass spectrometer operating in MALDI-TOF mode. Elemental analysis was performed on Vario EL cube. The ground-state geometries were optimized using the density functional with the B3LYP hybrid functional at the basis set level of 6-31G(d). All the calculations were performed using the Gaussian 09 package. UV spectra were measured on an HP 8453 spectrophotometer. Fluorescence spectra were recorded on a Hitachi F-4600 fluorescence spectrophotometer. TGA analysis was carried out on a TA TGA Q5000 under dry nitrogen at a heating rate of 10 °C min^{-1}. The fluorescence decay curves were recorded on an Edinburgh Instruments FLS920 combined with steady-state and time-resolved fluorescence spectrometers.

Devices Fabrication. The devices were fabricated on 80 nm-ITO coated glass with a sheet resistance of 25Ω/□. Prior to loading into the pretreatment chamber, the ITO-coated glass was soaked in ultrasonic detergent for 30 min, followed by spraying with deionized water for 10 min, soaking in ultrasonic deionized water for 30 min, and oven-baking for 1 h. The cleaned samples were treated by perfluoromethane plasma with a power of 100 W, a gas flow of 50 sccm, and a pressure of 0.2 Torr for 10 s in the pretreatment chamber. The samples were transferred to the organic chamber with a base pressure of 7×10^{-7} Torr for the deposition of NPB, emitter, and TPBi, which served as hole-transporting, light-emitting, and electron-transporting layers, respectively. The samples were then transferred to the metal chamber for cathode deposition, which was composed of lithium fluoride (LiF) capped with aluminum (Al). The light-emitting area was 4 mm^2. The current density−voltage characteristics of the devices were measured by an HP4145B semiconductor parameter analyzer. The forward direction photons emitted from the devices were detected by a calibrated UDT PIN-25D silicon photodiode. The luminance and external quantum efficiencies of the devices were inferred from the photocurrent of the photodiode. The EL spectra were obtained by a PR650 spectrophotometer. All measurements were carried out under air at room temperature without device encapsulation.

Preparation of Nanoaggregates. Stock THF solutions of the luminogens with a concentration of 10^{-4} M were prepared. Aliquots of the stock solution were transferred to 10 mL volumetric flasks. After appropriate amounts of THF were added, water was added dropwise under vigorous stirring to furnish 10^{-5} M solutions with different water contents (0−90 vol %). The PL measurements of the resultant solutions were then performed immediately.

Fluorescence Lifetime. The fluorescence decay curves were recorded on an Edinburgh Instruments FLS920 combined with steady-state and time-resolved fluorescence spectrometers. Decay of the PL intensity (I) with time (t) was fitted by a double-exponential function (eq 1), and the mean lifetime was calculated according to eq 2.

$$I = I_o + A_1\, e^{-t/\tau_1} + A_2\, e^{-t/\tau_2} \quad (1)$$

$$\langle\tau\rangle = (A_1\tau_1 + A_2\tau_2)/(A_1 + A_2) \quad (2)$$

Solvatochromic Effect. The influence of solvent polarity on the photophysical property of TPE-NB and TPE-PNPB can be understood using the Lippert−Mataga equation (eq 3), a model that describes the interaction between the solvent and the dipole moment of solute:

$$hc(\nu_a - \nu_f) = hc(\nu_a^o - \nu_f^o) - \frac{2(\mu_e - \mu_g)^2}{a^3} f(\varepsilon, n) \quad (3)$$

where $f(\varepsilon,n)$ is the orientational polarizability of solvents, ε and n are the solvent dielectric and the solvent refractive index, respectively, μ_e is the excited state dipole moment, and μ_g is the ground state dipole moment, a is the solvent cavity (Onsager) radius (6.67 and 7.09 Å for TPE-NB and TPE-PNPB, respectively), which is derived from the Avogadro number (N), molecular weight (M), and density (d = 1.0 g cm^{-3}). $f(\varepsilon,n)$ and a can be calculated respectively according to eq 4.

$$f(\varepsilon, n) = \frac{\varepsilon - 1}{2\varepsilon + 1} - \frac{n^2 - 1}{2n^2 + 1};\ a = (3M/4N\pi d)^{1/3} \quad (4)$$

Synthesis. *4-[2-(4-Bromophenyl)-1,2-diphenylvinyl]-N,N-diphenylaniline (**3**).* Into a 250 mL two-necked round-bottom flask with a reflux condenser was placed 1.75 g (5.0 mmol) of **1**, 3.92 g (15.0 mmol) of 4-bromo-benzophenone, and 2.60 g (40.0 mmol) of zinc dust. The flask was evacuated under a vacuum and flushed with dry

Scheme 1. Synthetic Routes to TPE-Bridged D-A Luminogens

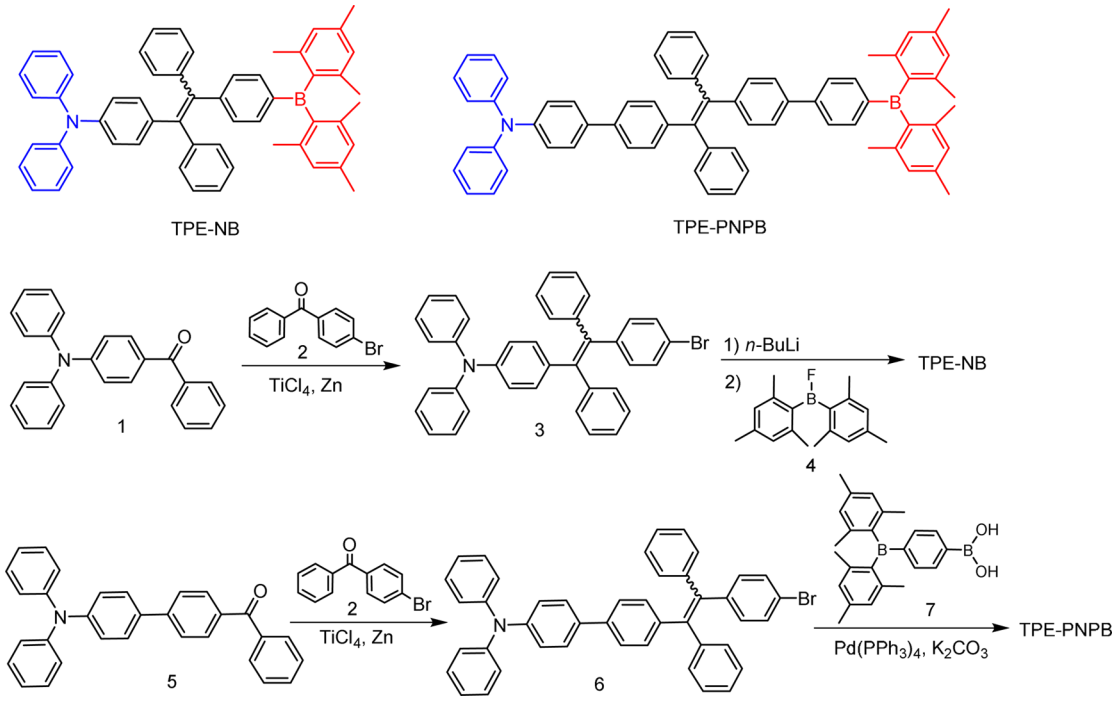

nitrogen three times, and then 100 mL of THF was added. After the mixture was cooled to −78 °C, 3.80 g (20.0 mmol) of $TiCl_4$ was then added dropwise by a syringe. After stirring for 15 min at −78 °C, the mixture was slowly warmed to room temperature and then was refluxed overnight. The mixture was quenched with 10% aqueous sodium carbonate and extracted with dichloromethane three times. The combined organic layers were washed with water and dried over anhydrous magnesium sulfate. After filtration and solvent evaporation, the crude product was purified by silica gel column chromatography. Green solid of **3** was isolated in 53% yield. ^{1}H NMR (600 MHz, $CDCl_3$), δ (ppm): 7.30−7.23 (m, 6H), 7.20−7.00 (m, 16H), 6.96−6.79 (m, 6H). ^{13}C NMR (150 MHz, $CDCl_3$), δ (ppm): 147.6, 147.5, 146.4, 146.2, 143.6, 143.2, 142.8, 141.5, 141.4, 139.2, 139.1, 137.5, 137.3, 133.1, 133.0, 132.1, 131.4, 131.3, 130.8, 129.2, 128.5, 128.4, 127.9, 127.8, 127.7, 126.7, 126.6, 124.4, 124.3, 122.9, 122.8, 122.7, 122.6, 120.3. HRMS (MALDI-TOF): m/z 577.1406 [M^+, calcd 577.1405].

*4′-[2-(4-Bromophenyl)-1,2-diphenylvinyl]-N,N-diphenyl-(1,1′-biphenyl)-4-amine (**6**).* The procedure was analogous to that described for compound **3**. Green solid, yield 50%. ^{1}H NMR (600 MHz, $CDCl_3$), δ (ppm): 7.49−7.45 (m, 2H), 7.39−7.33 (m, 2H), 7.30−7.24 (m, 6H), 7.18−7.03 (m, 20H), 6.97−6.92 (m, 2H). ^{13}C NMR (150 MHz, $CDCl_3$), δ (ppm): 147.7, 147.2, 143.5, 143.4, 143.3, 142.8, 142.0, 141.9, 141.3, 139.7, 138.6, 138.5, 134.5, 133.0, 131.7, 131.3, 131.0, 130.9, 129.3, 127.9, 127.8, 127.7, 127.5, 126.8, 126.7, 125.7, 124.4, 124.0, 122.9, 120.5, 120.4. HRMS (MALDI-TOF): m/z 653.1713 [M^+, calcd 653.1718].

4-{2-[4-(Dimesitylboranyl)phenyl]-1,2-diphenylvinyl}-N,N-diphenylaniline (TPE-NB). Into a 250 mL two-necked round-bottom flask was placed 1.74 g (3.0 mmol) of **3**. The flask was evacuated under a vacuum and flushed with dry nitrogen three times. Then, 80 mL of dry THF was added. The mixture was cooled to −78 °C, and 1.4 mL (2.4 M in hexane, 3.3 mmol) of *n*-BuLi was added dropwise by a syringe. The mixture was stirred for 2 h at −78 °C, and then 1.21 g (4.5 mmol) of dimesitylboron fluoride in 10 mL of THF was slowly injected to the reaction solution. The mixture was kept stirring for 1 h and warmed slowly to room temperature. The mixture was poured into water and extracted with dichloromethane three times. The combined organic layers were dried over anhydrous magnesium sulfate. After filtration and solvent evaporation, the crude product was purified by silica-gel column chromatography. Yellow solid of TPE-NB was obtained in 85% yield. ^{1}H NMR (400 MHz, CD_2Cl_2), δ (ppm): 7.26−7.18 (m, 6H), 7.15−6.99 (m, 18H), 6.89−6.84 (m, 2H), 6.79−6.71 (m, 6H), 2.28 (d, 6H), 1.95 (d, 12H). ^{13}C NMR (100 MHz, $CDCl_3$), δ (ppm): 147.5, 147.2, 147.0, 145.6, 142.9, 142.8, 142.7, 141.2, 141.0, 140.2, 139.9, 137.8, 137.1, 136.9, 135.1, 131.6, 130.8, 130.7, 130.3, 128.6, 128.5, 127.5, 127.0, 126.9, 126.0, 125.8, 123.8, 123.7, 123.6, 122.2, 122.1, 122.0, 121.8, 22.9, 22.8, 20.6. HRMS (MALDI-TOF): m/z 747.4032 [M^+, calcd 747.4036]. Anal. Calcd for $C_{56}H_{50}BN$: C, 89.94; H, 6.74; N, 1.87. Found: C, 90.25; H, 6.54; N, 1.86%.

4′-{2-[4′-(Dimesitylboranyl)-(1,1′-biphenyl)-4-yl]-1,2-diphenylvinyl}-N,N-diphenyl-(1,1′-biphenyl)-4-amine (TPE-PNPB). Into a 250 mL two-necked round-bottom flask was placed **6** (1.31 g, 2.0 mmol), **7** (1.11 g, 3.0 mmol), $Pd(PPh_3)_4$ (70 mg, 0.06 mmol), and Na_2CO_3 (848 mg, 8.0 mmol). The flask was evacuated under a vacuum and flushed with dry nitrogen three times, and then 80 mL of THF and 20 mL of water were added. The reaction mixture was refluxed for 24 h. After cooling to room temperature, the mixture was poured into water and extracted with dichloromethane three times. The combined organic layers were dried over anhydrous magnesium sulfate. After filtration and solvent evaporation, the crude product was purified by silica-gel column chromatography. Yellow solid of TPE-PNPB was isolated in 80% yield. ^{1}H NMR (400 MHz, $(CD_3)_2CO$)), δ (ppm): 7.70 (d, J = 8.0 Hz, 2H), 7.59−7.44 (m, 8H), 7.33−7.28 (m, 4H), 7.20−7.04 (m, 22H), 6.85 (d, J = 3.2 Hz, 4H), 2.28 (d, 6H), 2.01 (d, 12H). ^{13}C NMR (150 MHz, $CDCl_3$), δ (ppm): 147.7, 147.1, 144.5, 143.8, 143.6, 142.3, 141.8, 141.0, 140.8, 140.5, 138.6, 138.3, 138.2, 137.1, 134.6, 131.9, 131.8, 131.5, 129.3, 128.2, 127.8, 127.7, 127.5, 126.5, 126.4, 126.3, 126.2, 124.4, 124.0, 122.9, 114.9, 23.5, 21.3. HRMS (MALDI-TOF): m/z 899.4666 [M^+, calcd 899.4662]. Anal. Calcd for $C_{68}H_{58}BN$: C, 90.75; H, 6.50; N, 1.56. Found: C, 91.40; H, 6.49; N, 1.52%.

RESULTS AND DISCUSSION

Synthesis. Recently, the study on TPE-based materials has bloomed, generating numerous TPE derivatives with diverse functionalities. Most of them have a symmetrical structure, but unsymmetrical ones, particularly those substituted with donor and acceptor groups, are much more rare, probably due to synthetic difficulty.[37] In this work, unsymmetrical TPE derivatives, TPE-NB and TPE-PNPB, carrying diphenylamino

Table 1. Optical Properties, Thermal Stabilities, and Energy Levels of TPE-NB and TPE-PNPB

	λ_{abs} (nm)		λ_{em} (nm)				Φ_F[c](%)		T_g/T_d (°C)	HOMO/LUMO[d] (eV)	E_g (eV)
	CH[a]	film[b]	CH	THF	DMF	film	THF	film			
TPE-NB	380	391	505	515	544	526	0.2	64	107/271	−5.14/−2.34	2.80
TPE-PNPB	346	347	502	514	542	504	0.5	94	124/290	−5.18/−2.26	2.92

[a]Cyclohexane (CH). [b]Vacuum deposited film. [c]Fluorescence quantum yield in THF determined using quinine sulfate (Φ_F = 54.6% in 0.1 N sulfuric acid) as standard or in solid film by a calibrated intergrating sphere. [d]Determined by cyclic voltammetry.

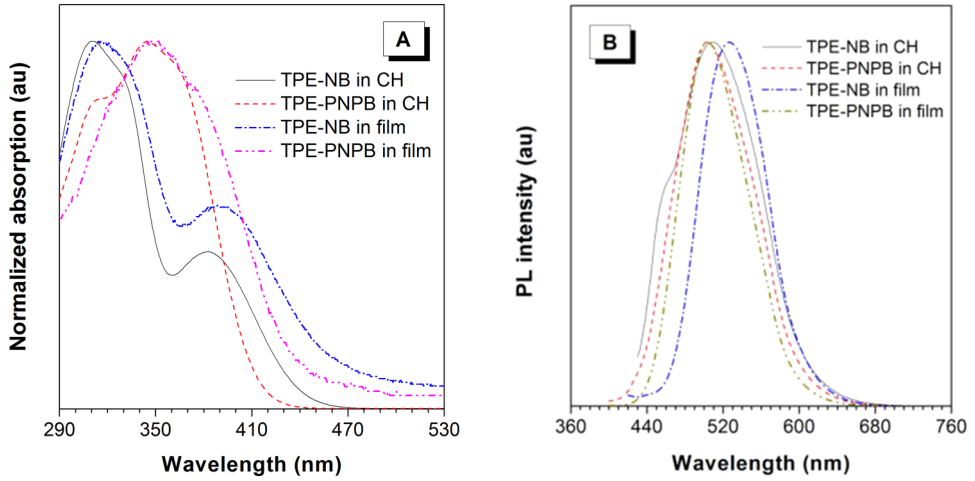

Figure 1. (A) Absorption and (B) PL spectra of TPE-NB and TPE-PNPB in cyclohexane (CH, 10 μM) and in solid films. Excitation wavelength: 360 nm.

and dimesitylboryl as donor and acceptor were prepared successfully in high yields according to the synthetic routes outlined in Scheme 1. Detailed procedures for the syntheses of intermediates and final products are described in the Experimental Section. Compounds **1**[38] and **5**[39] were prepared according to the methods published elsewhere. The key intermediates **3** and **6** were synthesized by cross McMurry couplings of 4-bromobenzophenone (**2**) with **1** and **5**, respectively. The treatment of **3** with *n*-butyllithium and, then, dimesitylboron fluoride (**4**) afforded target TPE-NB in 85% yield. The Suzuki coupling of **6** with [4-(dimesitylboranyl)phenyl]boronic acid (**7**) furnished TPE-PNPB in 80% yield. The new compounds were fully characterized by NMR, mass spectroscopy, and elemental analysis, with satisfactory results. The cross McMurry reaction gives stereorandom products with close contents of *cis*- and *trans*-isomers, which can hardly be separated, owing to their similar structural polarity as well as poor crystallization ability. They are soluble in common organic solvents including THF, dichloromethane, chloroform, toluene, etc., but insoluble in water. Their thermal properties were evaluated by thermogravimetric analysis (TGA) and differential scanning calorimetry (DSC) (Figure S1 and Table 1). TPE-NB and TPE-PNPB show high decomposition temperatures (T_d) of 271 and 290 °C, according to a 5% loss of initial weight, and high glass-transition temperatures (T_g) of 107 and 124 °C. These results disclose that they are thermally and morphologically stable, which enable them to function steadily as active layers in OLEDs.

Optical Property. The photophysical properties of TPE-NB and TPE-PNPB were measured using UV−visible absorption and PL spectroscopies. As illustrated in Figure 1A, TPE-NB exhibits a strong absorption band around 310 nm, mainly originated from the $\pi-\pi^*$ transition at the TPE moiety (Figure S2).[40] A characteristic long-wavelength absorption peak is observed at 380 nm for TPE-NB, which is assigned to the intramolecular charge transfer (CT) from electron-rich diphenylamino to electron-deficient dimesitylboryl. The absorption band from the CT state of TPE-PNPB is greatly blue-shifted to 346 nm and has partially merged with the absorption band of the $\pi-\pi^*$ transition of the backbone, implying that the electronic communication between diphenylamino and dimesitylboryl groups becomes much weaker.[41,42] In solid films, TPE-NB shows an absorption peak of the CT state at 391 nm, which is red-shifted by 11 nm in comparison with that in solution, while the absorption peak of TPE-PNPB is located at 347 nm, being almost identical to that in solution.

Like most TPE derivatives, both TPE-NB and TPE-PNPB show weak fluorescence in dilute THF solutions, and only faint PL signals peaking at 515 and 514 nm are recorded. Although the PL spectra of TPE-NB and TPE-PNPB consist of emissions from two isomers, the PL spectra are stable as their *cis* and *trans* isomers show similar emission behaviors, and their contents are also kept constant in the photophysical process. Their fluorescence quantum yields (Φ_F) in dilute THF solutions are as low as 0.2 and 0.5%, respectively, estimated using quinine sulfate (Φ_F = 54.6% in 0.1 N sulfuric acid) as a standard, disclosing that they are practically very weak emitters when dispersed in good solvents, which is attributed to the active intramolecular rotation (IMR) that deactivates the excitons in a nonradiative pathway. TPE-NB and TPE-PNPB fluoresce intensely when fabricated into solid films. The film of TPE-PNPB shows an emission maximum at 504 nm, which is blue-shifted by 10 nm relative to that in THF solution (Figure 1B). Such a kind of emission change between solid film and THF solution is often observed for many symmetrical TPE derivatives.[43,44] However, the film of TPE-NB shows strongly red-shifted emission at 526 nm, which appears to be

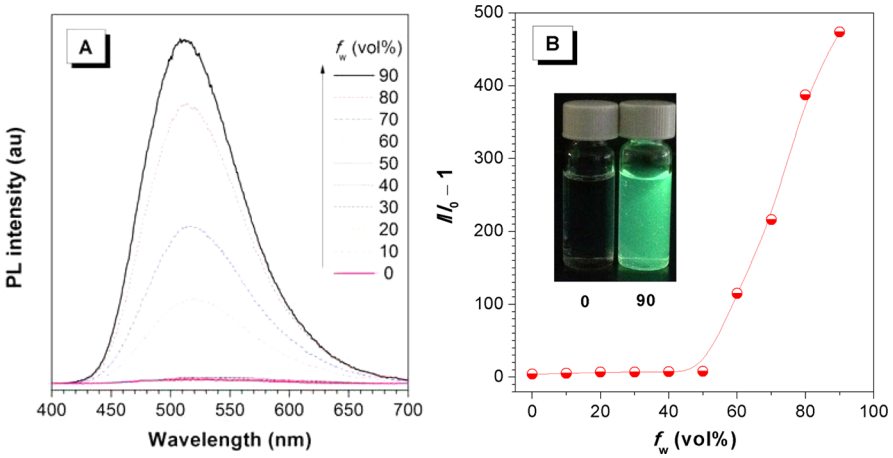

Figure 2. (A) PL spectra of TPE-PNPB in THF/water mixtures with different water fractions (f_w). (B) Plot of ($I/I_0 - 1$) values versus water fractions in THF/water mixtures of TPE-PNPB. I_0 is the PL intensity in pure THF solution. Inset: photos of TPE-PNPB in THF/water mixtures (f_w = 0 and 90%), taken under the illumination of a UV lamp (365 nm).

"abnormal." Concerning that the twisted molecular conformation plus branched dimesitylboryl group impede the close π-stacking of TPE-NB molecules in solid films, the chance to form strong $\pi-\pi$ intermolecular interactions should be little. Thereby, it is realized that the excited CT state of the D−A framework is responsible for the red-shifted PL in solid film. The films of TPE-NB and TPE-PNPB are highly fluorescent, owing to the restriction of the IMR process by the spatial constraint in the aggregated state. The Φ_F value of the film of TPE-NB is 64%, determined by integrating sphere, being 320-fold higher than that in solution. However, the value is lower than those of similar TPE derivatives carrying only one diphenylamino (97.6%)[43] or one dimesitylboryl (100%)[45] or two diphenylaminos (100%).[39,43] On the contrary, a much higher Φ_F value of 94% is measured from the film of TPE-PNPB. These results imply that the D−A interactions in TPE-NB and TPE-PNPB have exerted great influence on the emission wavelength and efficiency of the luminogens in solid films.

The noteworthy increase in Φ_F values of TPE-NB and TPE-PNPB from the solutions to the solid films suggests that they should possess AIE attributes. To further confirm this, their emission behaviors in THF/water mixtures were measured. Figure 2 depicts the PL spectra and emission intensity changes of TPE-PNPB as the addition of water to pure THF solution. It can be seen that whereas the emission remains weak when water content is low, the emission intensity enhances swiftly when water content gets high. Similar emission behaviors are also recorded from TPE-NB in THF/water mixtures (Figure S3). Since TPE-NB and TPE-PNPB are insoluble in water, their molecules must have aggregated in aqueous media. The IMR process hence is restricted, and the radiative decay of the excited state is promoted, enabling the molecules to emit strongly. These results manifest that both TPE-NB and TPE-PNPB are AIE-active indeed.

Solvatochromism. Generally, D−A substituted luminogens show a characteristic solvent-dependence in PL behavior, which arises from the rapid transition from the lowest optically allowed excited state (locally excited state, LE state) to a nonradiative intermediate state (CT state) upon photoexcitation. The CT state is readily formed in high-polar solvents, for it can be stabilized by a high-polar environment. Therefore, as the solvent polarity increases, the dipole moment of the molecule becomes larger, resulting in red-shifted emission and decreased emission intensity. The variation in PL emission of the luminogen is closely related to the change of molecular dipole moment, determined by external environment and intrinsic strengths of electron donor and acceptor.[46−48] Since TPE-NB and TPE-PNPB contain the same donor and acceptor groups, the interaction between them is thus sensitive to the conjugation and/or distance under the same conditions.

In an effort to explore the connection between the PL property and the molecular dipole moment, the ground and excited state dipole moments of TPE-NB and TPE-PNPB were calculated. The ground state dipole moments were 1.52 and 1.40 D for TPE-NB and TPE-PNPB, respectively, estimated from DFT calculation using the Gaussian 09 package at the basis set level of 6-31 G*. The dipole moment of the excited state can be determined from the slope of a plot of the Stokes shift ($\nu_a - \nu_f$) against the solvent parameters, or the orientation polarizability $\Delta f(\varepsilon,n)$, according to the Lippert−Mataga equation[49] (eq 1 in the Experimental Section). Detailed absorption and emission peak positions of TPE-NB and TPE-PNPB in solvents with different polarities at an identical concentration of 10^{-6} M are listed in Table S1 (Supporting Information). The experimental data do not appear to obey the linear relationship predicted by the Lippert−Mataga equation in the whole range of solvent polarity well (Figure 3). To make sure the calculated excited state dipole moments of TPE-NB and TPE-PNPB are authentic, we fit the line separately in the low-polarity region ($\Delta f < 0.20$) and high-polarity region ($\Delta f \geq 0.20$) following the recently reported method of Ma et al.[30] By analyzing the fitted line in the high-polarity region, excited state dipole moments are calculated to be 20.70 and 17.06 D for TPE-NB and TPE-PNPB, respectively. In the low-polarity region, the values are decreased to 5.97 and 5.02 D for TPE-NB and TPE-PNPB, respectively. The excited state dipole moment of TPE-NB is larger than that of TPE-PNPB, particularly in high-polar environments, demonstrating further that the D−A interaction is much weaker in TPE-PNPB than in TPE-NB.

The dipole moment derived from the D−A interaction influences the PL property of the luminogens not only in the solution state but also in the solid state. Chiang et al.[50] had demonstrated that the PL intensity is closely correlated with the local electric field induced by the molecular dipole moments of D−A luminogens. The strong local electric field facilitates

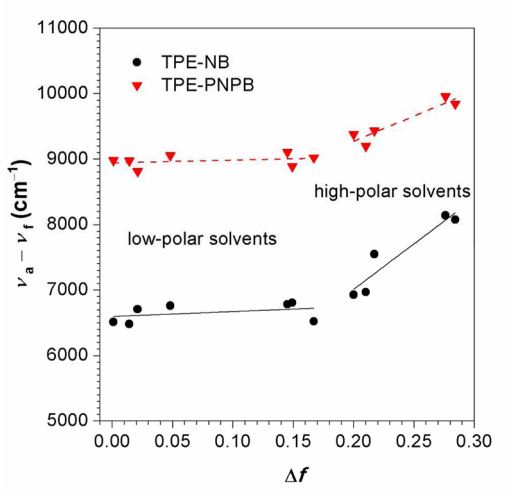

Figure 3. Linear correlation of orientation polarization (Δf) of solvent media with the Stokes shift ($\nu_a - \nu_f$) for TPE-NB (the solid lines) and TPE-PNPB (the dashed lines). The lines in the high- and low-polarity regions are fitted to the points with $\Delta f \geq 0.20$ and $\Delta f < 0.20$, respectively.

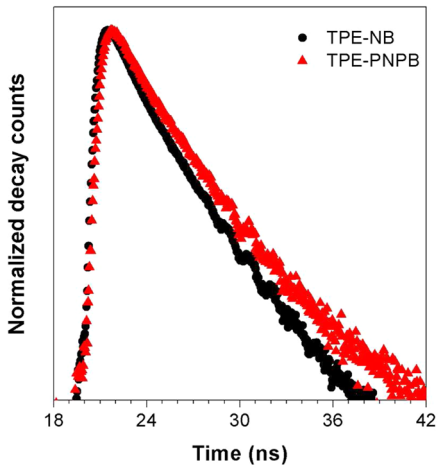

Figure 4. Fluorescence decay profiles of TPE-NB and TPE-PNPB in solid films, measured under ambient conditions. Excitation wavelength: 360 nm.

radiationless decay channels, leading to a high quenching rate in soild film. A similar fluorescence quenching effect by electric field had also been found by Nakabayashi et al.[51] when exerting an external electric field on the solid film of luminogen, which was attributed to the accelerated transition from the fluorescent LE state to the nonradiative CT state. Hence, to improve the solid-state emission efficiency, the influence of molecular dipole moment should be taken into careful consideration in the design of D−A substituted luminogens. To reveal the impact of dipole moment on the solid-state PL properties of TPE-NB and TPE-PNPB, their PL emissions in solutions and solid films are compared. The PL emission of TPE-PNPB in film (504 nm) is close to that in cyclohexane (CH, 502 nm), being bluer than that in THF (514 nm). On the contrary, the PL emission of TPE-NB in the film (526 nm) is red-shifted by 21 nm relative to that in CH (505 nm) and is similar to the emission in dichloromethane (525 nm, Table S1). As discussed above, in the excited state, TPE-PNPB has a much smaller dipole moment than TPE-NB. Hence, TPE-PNPB molecules are located in a low-polar environment and experience a weak electric field stemming from adjacent TPE-PNPB molecules in the condensed phase. These results evidence again that, in solid film, TPE-PNPB molecules are settled in a low-polar medium like in CH, but TPE-NB molecules are surrounded by high-polar molecules, just like in dichloromethane.[41,42] Therefore, the PL emission of TPE-PNPB is less quenched, rendering a much higher solid-state Φ_F value (94%) than that of TPE-NB (64%).

Fluorescence Decay. Fluorescence lifetime is an important kinetic parameter for the excited state decay process. It is closely associated with the strength of vibrational relaxation, and thus, fluorescence efficiency. To gain deeper insight into the PL properties of the present luminogens, a direct measurement of fluorescence decay profiles of the solid films was carried out (Figure 4). The singlet excited states of the films of TPE-NB and TPE-PNPB decay in a double-exponential fashion, and the singlet excited state lifetimes obtained by fitting decay profiles according to eq 1 (Experimental Section) are listed in Table 2. The mean lifetime (τ) of TPE-PNPB is calculated to be 2.69 ns at room temperature by eq 2 (Experimental Section), which is longer than that of TPE-NB (2.39 ns). On the basis of the fluorescence lifetimes, the excited state decay rates of TPE-NB and TPE-PNPB are calculated. According to quantum chemical calculations, Φ_F can be expressed as $\Phi_F = k_r/(k_r + k_{nr} + k_{isc})$, where k_r and k_{nr} are the radiative and nonradiative decay rates, respectively, and k_{isc} is the intersystem crossing rate from the singlet state to the triplet one. Since the spin−orbital coupling constant between S1 and lowest triplet excited state (T1) in these pure organic molecules is very small, the intersystem crossing process from S1 to T1 is negligible.[52−54] Thereby, Φ_F is simplified as $\Phi_F = k_r/(k_r + k_{nr})$. On the other hand, τ can be expressed as $\tau = 1/(k_r + k_{nr})$. Therefore, k_r is calculated to be 2.68×10^8 s^{-1} for TPE-NB and 3.49×10^8 s^{-1} for TPE-PNPB ($k_r = \Phi_F/\tau$). The k_{nr} of TPE-NB is 1.50×10^8 s^{-1}, which is much larger than that of TPE-PNPB (2.3×10^7 s^{-1}). The smaller k_r and larger k_{nr} of TPE-NB clearly evidence that the strong D−A interaction of TPE-NB exactly results in an acceleration of nonradiative relaxation and, thus, a notable decrease in solid-state PL efficiency.

Electronic Structures. To better understand the electronic structures of TPE-NB and TPE-PNPB, the optimized molecular structures and spatial distributions of HOMOs and LUMOs were calculated with the density function theory (DFT) method with a B3LYP/6-31G(d) basis set using the Gaussian 09 package. As illustrated in Figure 5, the dihedral angles of the biphenyl linkages in TPE-PNPB are 35°, suggesting that TPE-PNPB adopts a more twisted conformation than TPE-NB. The higher nonplanarity impairs the electronic coupling between diphenylamino and dimestylboryl groups in TPE-PNPB. In both luminogens, the diphenylamino contributes greatly to the HOMO, while the dimestylboryl is occupied by the LUMO (Figure 5). In contrast to TPE-NB, the spatial distributions of HOMO and LUMO are hardly overlapped in TPE-PNPB, which is attributed to its more twisted conformation and ineffective conjugation. The almost complete separation of HOMO and LUMO verifies that the D−A interaction in TPE-PNPB is weak, and thus, there is a small dipole moment in the excited state. On the other hand, it is preferable for efficient injection and transport of holes and

Table 2. Dipole Moments and Fluorescence Decay Times of TPE-NB and TPE-PNPB

		excited state dipole moment[b] (Debye)		fluorescence decay time[c] (ns)				
compounds	ground state dipole moment[a] (Debye)	$\Delta f < 0.20$	$\Delta f \geq 0.20$	τ_1	τ_2	τ^d	k_r^e (10^8 s^{-1})	k_{nr}^f (10^8 s^{-1})
TPE-NB	1.52	5.97	20.70	3.37	1.55	2.39	2.68	1.50
TPE-PNPB	1.40	5.02	17.06	3.23	2.15	2.69	3.49	0.23

[a]Calculated by B3LYP/6-31G*. [b]Calculated by Lippert-Mataga equation, Δf = orientational polarizability of solvents. [c]Recorded in the film state. [d]Calculated according to eq 2 in the Experimental Section. [e]Rate constant for radiative deactivation. [f]Rate constant for nonradiative deactivation.

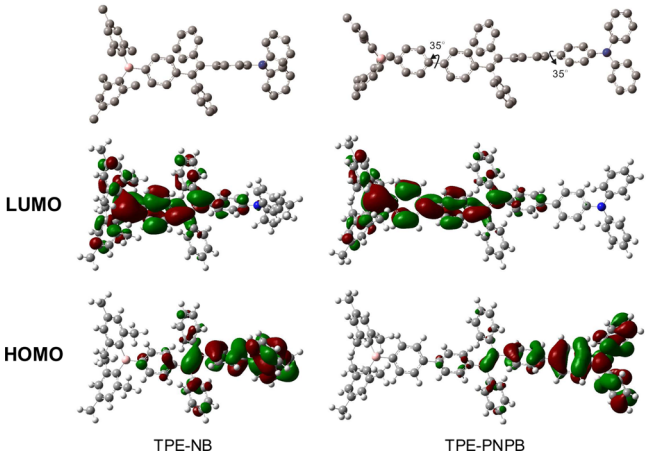

Figure 5. Optimized molecular structures in the ground state and molecular orbital amplitude plots of HOMOs and LUMOs of TPE-NB and TPE-PNPB, calculated by B3LYP/6-31G(d).

electrons in diphenylamino and dimestylboryl, respectively, which is beneficial to charge balance and exciton recombination in devices.[55]

Electrochemical Property. To evaluate the energy levels of both luminogens, their electrochemical properties were investigated by cyclic voltammetry (CV) in dichloromethane solution with 0.1 M tetrabutylammonium hexafluorophosphate as the supporting electrolyte at a scan rate of 50 mV s^{-1} using platinum as the working electrode and saturated calomel electrode (SCE) as the reference electrode. The cyclic voltammograms of TPE-NB and TPE-PNPB are given in Figure S4. The energy levels of HOMO [HOMO = −(4.4 + E_{onset})] and LUMO [LUMO = −(HOMO + E_g)] were determined by the onset potential of oxidation (E_{onset}) and optical band gap. The HOMO energy levels of TPE-NB and TPE-PNPB are calculated to be −5.14 and −5.18 eV, which are higher than that of 1,4-bis[(1-naphthylphenyl)amino]biphenyl (NPB; −5.3 eV),[56] indicating that the hole injection is favored in both luminogens. The LUMO energy levels of TPE-NB and TPE-PNPB are −2.34 and −2.26 eV, being close to that of NPB (−2.3 eV) but higher than that of 1,3,5-tris(*N*-phenylbenzimidazol-2-yl)benzene (TPBi; −2.7 eV).[57]

Electroluminescence. Given the high solid-state emission efficiencies, TPE-NB and TPE-PNPB were subjected to an EL study in undoped OLEDs. Trilayer OLEDs with a configuration of ITO/NPB (60 nm)/emitter (20 nm)/TPBi (40 nm)/LiF (1 nm)/Al (100 nm) (device I) were fabricated, in which TPE-NB and TPE-PNPB served as a light-emitting layer (EML), NPB acted as a hole-transporting layer (HTL), and TPBi functioned as an electron-transporting layer (ETL). The current−voltage−luminance characteristics and efficiency curves of devices I are depicted in Figure 6, and the relevant performance data are summarized in Table 3. The EL emission of TPE-PNPB is located at 516 nm, which is red-shifted by 12 nm relative to the PL in film (504 nm). TPE-NB shows a much redder EL emission at 544 nm, with a stronger red-shift of 18 nm in comparison with its PL in film (526 nm). Device I of TPE-PNPB shows a low turn-on voltage (V_{on}) of 3.2 V, and a maximum luminance (L_{max}) of 49 993 cd m^{-2}, which are similar to those of TPE-NB-based device I (V_{on} = 3.3 V, L_{max} = 42 924 cd m^{-2}). However, the EL efficiencies of TPE-PNPB-based device I are much superior to those of TPE-NB-based one. Excellent maximum current (η_c), power (η_p), and external quantum (η_{ext}) efficiencies of 15.7 cd A^{-1}, 12.9 lm W^{-1}, and 5.12% are attained by device I of TPE-PNPB, which are much higher than those of device I of TPE-NB (10.5 cd A^{-1}, 9.4 lm W^{-1}, and 3.24%). Significantly, the device shows very small efficiency roll-off as the increase of luminance, affording a high $\eta_{ext,1000}$ of 4.75% at a luminance of 1000 cd m^{-2}. These results demonstrate the great potential of TPE-PNPB as a light emitter for undoped OLEDs.

Previous studies had shown that the collaboration of TPE with electron donors, such as triphenylamine (TPA), carbazozle, etc., furnished luminescent materials with good hole-transporting ability.[38−40,43,44,58] However, the highest external quantum efficiency of bilayer OLEDs utilizing them as both a light emitter and a hole transporter is 4.5% so far,[40] leaving much room for further improvement. Considering the high-lying HOMO energy levels of TPE-NB and TPE-PNPB, it is envisioned that they may also function as hole transporters in addition to light emitters in devices. To confirm the bifunctionality of the luminogens, bilayer OLEDs with a configuration of ITO/emitter (80 nm)/TPBi (40 nm)/LiF (1 nm)/Al (100 nm) (device II) were fabricated, in which TPE-NB and TPE-PNPB served as both EML and HTL, and TPBi acted as ETL. Devices II of TPE-NB and TPE-PNPB show similar low turn-on voltages and radiate the same EL emissions as device I. The EL efficiencies of device II, however, are advanced relative to those of device I (Table 3). TPE-PNPB shows better performances than TPE-NB in device II. The η_c, η_p, and η_{ext} of device II of TPE-PNPB reach 16.2 cd A^{-1}, 14.4 lm W^{-1}, and 5.35%, being much higher than those of device I of TPE-NB (11.9 cd A^{-1}, 9.90 lm W^{-1}, and 3.73%). Device II also shows small roll-offs in ambient air. A high $\eta_{ext,1000}$ of 4.45% is retained at a luminance of 1000 cd m^{-2} in device II of TPE-PNPB.

TPE-NB and TPE-PNPB are similar in molecular structure, but their EL emissions differ greatly from each other. The difference in EL maxima (28 nm) is even larger than that in PL maxima (22 nm). To verify that the EL emissions are stemmed from TPE-NB and TPE-PNPB rather than exciplexes formed at interfaces, another kind of bilayer OLEDs with a configuration of ITO/NPB (60 nm)/emitter (60 nm)/LiF (1 nm)/Al (100 nm) (device III) were fabricated, in which TPE-NB and TPE-PNPB served as both EML and ETL, and NPB acted as HTL. As shown in Figure S5, in devices I−III, TPE-NB and TPE-

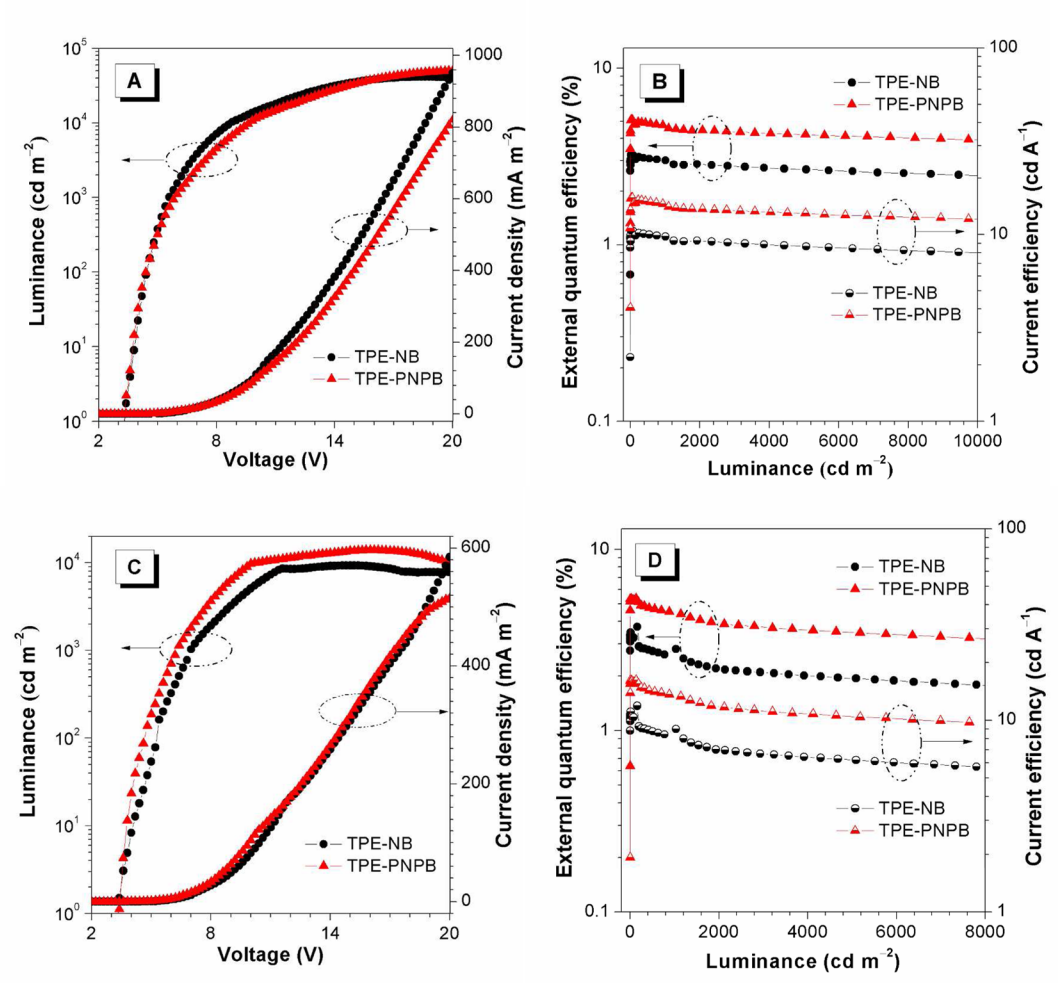

Figure 6. (A) Current density−voltage−luminance characteristics and (B) external quantum efficiencies and current efficiencies with the luminance of device I. (C) Current density−voltage−luminance characteristics and (D) external quantum efficiencies and current efficiencies with the luminance of device II. Device configuration: ITO/NPB (60 nm)/emitter (20 nm)/TPBi (40 nm)/LiF (1 nm)/Al (100 nm) (device I); ITO/emitter (80 nm)/TPBi (40 nm)/LiF (1 nm)/Al (100 nm) (device II).

Table 3. EL Performances of OLEDs Based on TPE-NB and TPE-PNPB[a]

emitter	device	V_{on} (V)	λ_{EL} (nm)	L_{max} (cd m^{-2})	η_c (cd A^{-1})	η_{ext} (%)	η_p (lm W^{-1})	$\eta_{c,1000}$ (cd A^{-1})	$\eta_{ext,1000}$ (%)	CIE (x, y)
TPE-NB	I	3.3	544	42924	10.5	3.24	9.40	9.07	2.79	0.35, 0.55
	II	3.3	544	7942	11.9	3.73	9.90	8.24	2.62	0.37, 0.54
TPE-PNPB	I	3.2	516	49993	15.7	5.12	12.9	14.6	4.75	0.27, 0.51
	II	3.2	516	13678	16.2	5.35	14.4	13.4	4.45	0.25, 0.50

[a]Device configuration: ITO/NPB (60 nm)/emitter (20 nm)/TPBi (40 nm)/LiF (1 nm)/Al (100 nm) (device I); ITO/emitter (80 nm)/TPBi (40 nm)/LiF (1 nm)/Al (100 nm) (device II). Abbreviations: λ_{EL} = EL maximum, V_{on} = turn-on voltage at 1 cd m^{-2}, L_{max} = maximum luminance, η_c = maximum current efficiency, $\eta_{c,1000}$ = current efficiency at 1000 cd m^{-2}, η_{ext} = maximum external quantum efficiency, $\eta_{ext,1000}$ = external quantum efficiency at 1000 cd m^{-2}, η_p = maximum power efficiency, CIE = Commission Internationale de l'Eclairage coordinates.

PNPB show quite similar EL spectra with the same EL maxima of 544 and 516 nm, respectively. These results exclude the exciplex formation between emitter/TPBi or NPB/emitter layers and confirm that the EL emissions came from TPE-NB and TPE-PNPB indeed. Since in EL devices, the electric field should be much stronger than that induced by the dipole moment of the molecules, the excited dipole moments under electrical excitation are reasonably larger than those in solid films under photoexcitation, which results in red-shifted EL emissions. Since TPE-PNPB possesses a weaker D−A interaction than TPE-NB, the excited dipole moment is smaller than that of TPE-NB, leading to a smaller red-shift in EL emission.

Through calculation from the relationship $\eta_{ext} = \eta_{int}\cdot\eta_{ph}$, assuming a light out-coupling efficiency of $\eta_{ph} \approx 1/(2n^2) \approx$ 20% for a glass substrate with an index of refraction n = 1.5, the η_{ext} (5.35%) corresponds to an internal quantum efficiency η_{int} of 26.8% (η_{ext}/η_{ph}).[30] Given a solid-state Φ_F of 94%, it is calculated that about 28% (η_{int}/Φ_F) of excitons formed by electron−hole recombination undergo radiative decay in device II of TPE-PNPB. By the same method, a close value of 29% is also obtained for the radiatively deactivated excitons in device II of TPE-NB. The radiative exciton ratios in devices of both

luminogens exceed the limit of 25% spin statistics, presumably due to the HLCT mechanism.[30] Since the excitons participating in the radiation process are similar, the solid-state Φ_F value thus become a decisive factor to determine the EL efficiency of the device. Therefore, it is quite understandable that the devices of TPE-PNPB are more efficient than those of TPE-NB because the Φ_F value of the TPE-PNPB film is much higher than that of the TPE-NB film.

Concerning highlighted EL efficiencies of device II utilizing TPE-PNPB as both HTL and EML, good hole mobility should be another crucial factor, in addition to high solid-state emission efficiency and matched HOMO energy levels between TPE-PNPN and NPB as discussed above (Figure 7). To prove

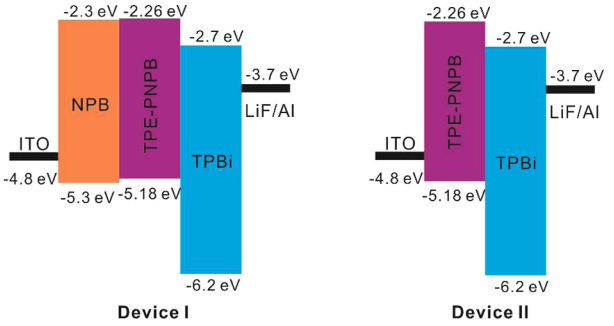

Figure 7. Energy level diagrams of multilayer EL devices of TPE-PNPB with or without NPB as a hole-transporting layer.

this, the hole-transporting abilities of the films of TPE-PNPB and NPB are compared by means of the space-charge-limited current technique. As the voltage is increased, the current becomes space-charge limited with a nearly quadratic dependence on voltage, and the electrical characteristics can be expressed by the Mott–Gurney equation and the Pool–Frenkel formalism (Experimental Section). Figure 8 illustrates the

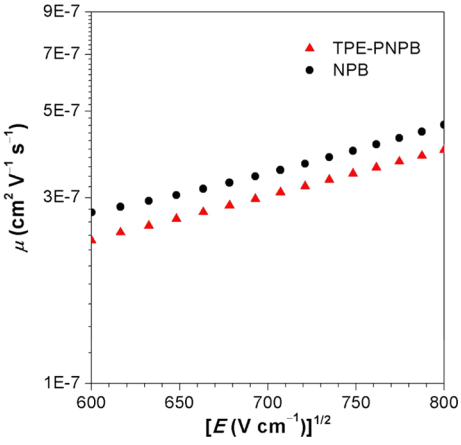

Figure 8. Electric field dependence of the hole mobility (μ) for the solid films of TPE-PNPB and NPB, measured from hole only devices with a configuration of ITO/MoO_3 (6 nm)/TPE-PNPB or NPB (200 nm)/MoO_3 (8 nm)/Al at room temperature.

obtained electric field dependence of the hole mobility (μ) for the solid films, measured from hole only devices with a configuration of ITO/MoO_3 (6 nm)/TPE-PNPB or NPB (200 nm)/MoO_3 (8 nm)/Al. Obviously, the mobility values of TPE-PNPB and NPB are almost at the same level. The excellent hole-transporting ability enables TPE-PNPB to act as an efficient bifunctional material in bilayer OLEDs without sacrificing the device performances. On the other hand, the presence of electron deficient dimesitylboryl facilitates the electron injection and transport, leading to more balanced holes and electrons in devices. Therefore, although the device configuration is far from optimal, the EL efficiency of 5.35% obtained in ambient air by the present bilayer device of TPE-PNPB is advanced obviously relative to those of reported bilayer devices based on symmetrical linear (4.4%)[43] or starburst (4.5%)[40] adducts of TPE and triphenylamine.

CONCLUSIONS

The rational design of luminescent molecules is of significant importance to achieve efficient solid-state PL emission and good carrier transport, which are essential for the fabrication of high-performance OLEDs. In this work, two thermally stable TPE derivatives (TPE-NB and TPE-PNPB) carrying diphenylamino and dimesitylboryl as electron donor and acceptor are synthesized and characterized. The impacts of D–A interaction on the PL and EL properties of the luminogens are investigated in detail. TPE-NB shows strong D–A interaction with a characteristic absorption peak associated with the CT state, while TPE-PNPB exhibits weak D–A interaction with a greatly blue-shifted absorption band from the CT state. Both luminogens show AIE characteristics and fluoresce strongly in solid films, with high Φ_F values up to 94%. TPE-PNPB shows improved PL and EL properties relative to TPE-NB. A remarkably high external quantum efficiency of 5.35% is obtained in ambient air when TPE-PNPB is utilized as both EML and HTL in the bilayers OLEDs without thorough optimization. The excellent EL efficiencies from a simplified device should be highlighted, which is preferable to reduce manufacturing costs of devices. More importantly, it is found that strong D–A interaction provokes a decrease in PL and EL efficiencies by virtue of the intensification of nonradiative relaxation in this system. These results virtually demonstrate an effective design strategy for achieving efficient multifunctional light emitters for undoped OLEDs and encourage further extensive investigation of the key role of D–A interaction in the determination of device performance.

ASSOCIATED CONTENT

Supporting Information

Tables of absorption and emission data, thermal analysis, absorption of TPE and TPE-PP, AIE properties of TPE-NB, Cyclic voltammograms of TPE-NB and TPE-PNPB, and EL spectra of TPE-NB and TPE-PNPB in different devices. This material is available free of charge via the Internet at http://pubs.acs.org.

AUTHOR INFORMATION

Corresponding Authors

*E-mail: zujinzhao@gmail.com.
*E-mail: tangbenz@ust.hk.

Notes

The authors declare no competing financial interest.

ACKNOWLEDGMENTS

We acknowledge financial support from the National Natural Science Foundation of China (51273053 and 21104012), the National Basic Research Program of China (973 Program, 2013CB834702), the Fundamental Research Funds for the

Central Universities (2013ZZ0002), the Guangdong Innovative Research Team Program of China (20110C0105067115), and the Research Grants Council of Hong Kong (HKUST2/CRF/10).

REFERENCES

(1) Shih, P. I.; Chuang, C. Y.; Chien, C. H.; Diau, E. W. G.; Shu, C. F. Highly Efficient Non-Doped Blue-Light-Emitting Diodes Based on an Anthrancene Derivative End-Capped with Tetraphenylethylene Groups. *Adv. Funct. Mater.* **2007**, *17*, 3141−3146.

(2) Grimsdale, A. C.; Chan, K.; Martin, R. E.; Jokisz, P. G.; Holmes, A. B. Synthesis of Light-Emitting Conjugated Polymers for Applications in Electroluminescent Devices. *Chem. Rev.* **2009**, *109*, 897−1091.

(3) Anthony, J. E.; Facchetti, A.; Heeney, M.; Marder, S. R.; Zhan, X. n-Type Organic Semiconductors in Organic Electronics. *Adv. Mater.* **2010**, *22*, 3876−3892.

(4) Duan, L.; Qiao, J.; Sun, Y.; Qiu, Y. Strategies to Design Bipolar Small Molecules for OLEDs: Donor-Acceptor Structure and Non-Donor-Acceptor Structure. *Adv. Mater.* **2011**, *23*, 1137−1144.

(5) Zhao, Z.; Li, J. H.; Lu, P.; Yang, Y. Fluorescent, Carrier-Trapping Dopants for Highly Efficient Single-Layer Polyfluorene LEDs. *Adv. Funct. Mater.* **2007**, *17*, 2203−2210.

(6) Moorthy, J. N.; Venkatakrishnan, P.; Natarajan, P.; Huang, D. F.; Chow, T. J. De Novo Design for Functional Amorphous Materials: Synthesis and Thermal and Light-Emitting Properties of Twisted Anthracene-Functionalized Bimesitylenes. *J. Am. Chem. Soc.* **2008**, *130*, 17320−17333.

(7) Chen, C. H. Evolution of Red Organic Light-Emitting Diodes: Materials and Devices. *Chem. Mater.* **2004**, *16*, 4389−4400.

(8) Bi, H.; Ye, K.; Zhao, Y.; Yang, Y.; Liu, Y.; Wang, Y. Fluorinated Quinacridone Derivative Based Organic Light-Emitting Device with High Power Efficiency. *Org. Electron.* **2010**, *11*, 1180−1184.

(9) Gong, X.; Wang, S.; Moses, D.; Bazan, G. C.; Heeger, A. J. Multilayer Polymer Light-Emitting Diodes: White-Light Emission with High Efficiency. *Adv. Mater.* **2005**, *17*, 2053−2058.

(10) Luo, J.; Xie, Z.; Lam, J. W. Y.; Cheng, L.; Chen, H.; Qiu, C.; Kwok, H. S.; Zhan, X.; Liu, Y.; Zhu, D.; Tang, B. Z. Aggregation-Induced Emission of 1-Methyl-1,2,3,4,5-pentaphenylsilole. *Chem. Commun.* **2001**, 1740−1741.

(11) Hong, Y.; Lam, J. W. Y.; Tang, B. Z. Aggregation-Induced Emission. *Chem. Soc. Rev.* **2011**, *40*, 5361−5388.

(12) Zhao, Z.; Wang, Z.; Lu, P.; Chan, C. Y. K.; Liu, D.; Lam, J. W. Y.; Sung, H. H. Y.; Williams, I. D.; Ma, Y.; Tang, B. Z. Structural Modulation of Solid-State Emission of 2,5-Bis(trialkylsilylethynyl)-3,4-diphenylsiloles. *Angew. Chem., Int. Ed.* **2009**, *121*, 7744−7747.

(13) Li, Z.; Dong, Y.; Mi, B.; Tang, Y.; Häussler, M.; Tong, H.; Dong, Y.; Lam, J. W. Y.; Ren, Y.; Sun, H. H. Y.; Wong, K. S.; Gao, P.; Williams, I. D.; Kwok, H. S.; Tang, B. Z. Structural Control of the Photoluminescence of Silole Regioisomers and Their Utility as Sensitive Regiodiscriminating Chemosensors and Efficient Electroluminescent Materials. *J. Phys. Chem. B* **2005**, *109*, 10061−10066.

(14) Zhao, Z.; He, B.; Nie, H.; Chen, B.; Lu, P.; Qin, A.; Tang, B. Z. Stereoselective Synthesis of Folded Luminogens with Arene-Arene Stacking Interactions and Aggregation-Enhanced Emission. *Chem. Commun.* **2014**, *50*, 1131−1133.

(15) Zhao, Z.; Chen, S.; Lam, J. W. Y.; Lu, P.; Zhong, Y.; Wong, K. S.; Kwok, H. S.; Tang, B. Z. Creation of Highly Efficient Solid Emitter by Decorating Pyrene Core with AIE-Active Tetraphenylethene Peripheries. *Chem. Commun.* **2010**, *46*, 2221−2223.

(16) Yuan, W. Z.; Lu, P.; Chen, S.; Lam, J. W. Y.; Wang, Z.; Liu, Y.; Kwok, H. S.; Ma, Y.; Tang, B. Z. Changing the Behavior of Chromophores from Aggregation-Caused Quenching to Aggregation-Induced Emission: Development of Highly Efficient Light Emitters in the Solid State. *Adv. Mater.* **2010**, *22*, 2159−2163.

(17) Zhao, Z.; Lu, P.; Lam, J. W. Y.; Wang, Z.; Chan, C. Y. K.; Sung, H. H. Y.; Williams, I. D.; Ma, Y.; Tang, B. Z. Molecular Anchors in the Solid State: Restriction of Intramolecular Rotation Boosts Emission Efficiency of Luminogen Aggregates to Unity. *Chem. Sci.* **2011**, *2*, 672−675.

(18) Chen, L.; Jiang, Y.; Nie, H.; Lu, P.; Sung, H. H. Y.; Williams, I. D.; Kwok, H. S.; Huang, F.; Qin, A.; Zhao, Z.; Tang, B. Z. Creation of Bifunctional Materials: Improve Electron-Transporting Ability of Light Emitters Based on AIE-Active 2,3,4,5-Tetraphenylsiloles. *Adv. Funct. Mater.* **2014**, *24*, 3621−3630.

(19) Huang, J.; Sun, N.; Dong, Y.; Tang, R.; Lu, P.; Cai, P.; Li, Q.; Ma, D.; Qin, J.; Li, Z. Similar or Totally Different: The Control of Conjugation Degree through Minor Structural Modifications, and Deep-Blue Aggregation-Induced Emission Luminogens for Non-Doped OLEDs. *Adv. Funct. Mater.* **2013**, *23*, 2329−337.

(20) Du, X.; Qi, J.; Zhang, Z.; Ma, D.; Wang, Z. Y. Efficient Non-doped Near Infrared Organic Light-Emitting Devices Based on Fluorophores with Aggregation-Induced Emission Enhancement. *Chem. Mater.* **2012**, *24*, 2178−2185.

(21) Li, J.; Duan, Y.; Li, Q. Novel Thieno-[3, 4-*b*]-pyrazine Derivatives for Non-doped Red Organic Light-Emitting Diodes. *Dyes Pigments* **2013**, *96*, 391−396.

(22) Huang, J.; Tang, R.; Zhang, T.; Li, Q.; Yu, G.; Xie, S.; Liu, Y.; Ye, S.; Qin, J.; Li, Z. A New Approach to Prepare Efficient Blue AIE Emitters for Undoped OLEDs. *Chem.—Eur. J.* **2014**, *20*, 5317−5326.

(23) Mu, G.; Zhang, W.; Xu, P.; Wang, H.; Wang, Y.; Wang, L.; Zhuang, S.; Zhu, X. Constructing New n-Type, Ambipolar, and p-Type Aggregation-Induced Blue Luminogens by Gradually Tuning the Proportion of Tetrahphenylethene and Diphenylphophine Oxide. *J. Phys. Chem. C* **2014**, *118*, 8610−8616.

(24) Shirota, Y.; Kinoshita, M.; Noda, T.; Okumoto, K.; Ohara, T. A Novel Class of Emitting Amorphous Molecular Materials as Bipolar Radical Formants: 2-{4-[Bis(4-methylphenyl)amino]phenyl}- 5-(dimesitylboryl)thiophene and 2-{4-[Bis(9,9-dimethylfluorenyl)-amino]phenyl}- 5-(dimesitylboryl)thiophene. *J. Am. Chem. Soc.* **2000**, *122*, 11021−11022.

(25) Chen, C.-T.; Wei, Y.; Lin, J.-S.; Moturu, M. V. R. K.; Chao, W.-S.; Tao, Y.-T.; Chien, C.-H. Doubly Ortho-Linked Quinoxaline/Diphenylfluorene Hybrids as Bipolar, Fluorescent Chameleons for Optoelectronic Applications. *J. Am. Chem. Soc.* **2006**, *128*, 10992−10993.

(26) Beverina, L.; Pagani, G. A. π-Conjugated Zwitterions as Paradigm of Donor−Acceptor Building Blocks in Organic-Based Materials. *Acc. Chem. Res.* **2013**, *47*, 319−329.

(27) Chen, S.; Xu, X.; Liu, Y.; Yu, G.; Sun, X.; Qiu, W.; Ma, Y.; Zhu, D. Synthesis and Characterization of n-Type Materials for Non-Doped Organic Red-Light-Emitting Diodes. *Adv. Funct. Mater.* **2005**, *15*, 1541−1546.

(28) Uoyama, H.; Goushi, K.; Shizu, K.; Nomura, H.; Adachi, C. Highly Efficient Organic Light-Emitting Diodes from Delayed Fluorescence. *Nature* **2012**, *492*, 234−238.

(29) Dias, F. B.; Bourdakos, K. N.; Jankus, V.; Moss, K. C.; Kamtekar, K. T.; Bhalla, V.; Santos, J.; Bryce, M. R.; Monkman, A. P. Triplet Harvesting with 100% Efficiency by Way of Thermally Activated Delayed Fluorescence in Charge Transfer OLED Emitters. *Adv. Mater.* **2013**, *25*, 3707−3714.

(30) Li, W.; Liu, D.; Shen, F.; Ma, D.; Wang, Z.; Feng, T.; Xu, Y.; Yang, B.; Ma, Y. A Twisting Donor-Acceptor Molecule with an Intercrossed Excited State for Highly Efficient, Deep-Blue Electroluminescence. *Adv. Funct. Mater.* **2012**, *22*, 2797−2803.

(31) Zhao, Z.; Lam, J. W. Y.; Tang, B. Z. Tetraphenylethene: a Versatile AIE Building Block for the Construction of Efficient Luminescent Materials for Organic Light-Emitting Diodes. *J. Mater. Chem.* **2012**, *22*, 23726−23740.

(32) Zhao, Z.; Deng, C.; Chen, S.; Lam, J. W. Y.; Qin, W.; Lu, P.; Wang, Z.; Kwok, H. S.; Ma, Y.; Qiu, H.; Tang, B. Z. Full Emission Color Tuning in Luminogens Constructed from Tetraphenylethene, Benzo-2,1,3-thiadiazole and Thiophene Building Blocks. *Chem. Commun.* **2011**, *47*, 8847−8849.

(33) Kinoshita, M.; Kita, H.; Shirota, Y. A Novel Family of Boron-Containing Hole-Blocking Amorphous Molecular Materials for Blue-

and Blue−Violet-Emitting Organic Electroluminescent Devices. *Adv. Funct. Mater.* **2002**, *12*, 780−786.
(34) Wakamiya, A.; Mori, K.; Yamaguchi, S. 3-Boryl-2,2′-bithiophene as a Versatile Core Skeleton for Full-Color Highly Emissive Organic Solids. *Angew. Chem., Int. Ed.* **2007**, *46*, 4273−4276.
(35) Entwistle, C. D.; Marder, T. B. Applications of Three-Coordinate Organoboron Compounds and Polymers in Optoelectronics. *Chem. Mater.* **2004**, *16*, 4574−4585.
(36) Jia, W. L.; Feng, X. D.; Bai, D. R.; Lu, Z. H.; Wang, S.; Vamvounis, G. Mes_2B(*p*-4,4′-biphenyl-NPh(1-naphthyl)): A Multifunctional Molecule for Electroluminescent Devices. *Chem. Mater.* **2004**, *17*, 164−170.
(37) Gu, X.; Yao, J.; Zhang, G.; Zhang, C.; Yan, Y.; Zhao, Y.; Zhang, D. New Electron-Donor/Acceptor-Substituted Tetraphenylethylenes: Aggregation-Induced Emission with Tunable Emission Color and Optical-Waveguide Behavior. *Chem.—Asian J.* **2013**, *8*, 2362−2369.
(38) Liu, Y.; Chen, X.; Lv, Y.; Chen, S.; Lam, J. W. Y.; Mahtab, F.; Kwok, H. S.; Tao, X.; Tang, B. Z. Systemic Studies of Tetraphenylethene−Triphenylamine Oligomers and a Polymer: Achieving Both Efficient Solid-State Emissions and Hole-Transporting Capability. *Chem.—Eur. J.* **2012**, *18*, 9929−9938.
(39) Zhao, Z.; Li, Z.; Lam, J. W. Y.; Maldonado, J.-L.; Ramos-Ortiz, G.; Liu, Y.; Yuan, W.; Xu, J.; Miao, Q.; Tang, B. Z. High Hole Mobility of 1,2-Bis[4-(diphenylamino)biphenyl-4-yl]-1,2-diphenylethene in Field Effect Transistor. *Chem. Commun.* **2011**, *47*, 6924−6926.
(40) Kim, J. Y.; Yasuda, T.; Yang, Y. S.; Adachi, C. Bifunctional Star-Burst Amorphous Molecular Materials for OLEDs: Achieving Highly Efficient Solid-State Luminescence and Carrier Transport Induced by Spontaneous Molecular Orientation. *Adv. Mater.* **2013**, *25*, 2666−2671.
(41) Zhang, Q.; Li, B.; Huang, S.; Nomura, H.; Tanaka, H.; Adachi, C. Efficient Blue Organic Light-Emitting Diodes Employing Thermally Activated Delayed Fluorescence. *Nat. Photonics* **2014**, *8*, 326−332.
(42) Hu, J.-Y.; Pu, Y.-J.; Satoh, F.; Kawata, S.; Katagiri, H.; Sasabe, H.; Kido, J. Bisanthracene-Based Donor−Acceptor-type Light-Emitting Dopants: Highly Efficient Deep-Blue Emission in Organic Light-Emitting Devices. *Adv. Funct. Mater.* **2014**, *24*, 2064−2071.
(43) Liu, Y.; Chen, S.; Lam, J. W. Y.; Lu, P.; Kwok, R. T. K.; Mahtab, F.; Kwok, H. S.; Tang, B. Z. Tuning the Electronic Nature of Aggregation-Induced Emission Luminogens with Enhanced Hole-Transporting Property. *Chem. Mater.* **2011**, *23*, 2536−2544.
(44) Qin, W.; Liu, J.; Chen, S.; Lam, J. W. Y.; Arseneault, M.; Yang, Z.; Zhao, Q.; Kwok, H. S.; Tang, B. Z. Crafting NPB with Tetraphenylethene: A Win−Win Strategy to Create Stable and Efficient Solid-State Emitters with Aggregation-Induced Emission Feature, High Hole-Transporting Property and Efficient Electroluminescence. *J. Mater. Chem.* **2014**, *2*, 3756−3761.
(45) Yuan, W. Z.; Chen, S.; Lam, J. W. Y.; Deng, C.; Lu, P.; Sung, H. H. Y.; Williams, I. D.; Kwok, H. S.; Zhang, Y.; Tang, B. Z. Towards High Efficiency Solid Emitters with Aggregation-Induced Emission and Electron-Transport Characteristics. *Chem. Commun.* **2011**, *47*, 11216−11218.
(46) Rettig, W. Charge Separation in Excited States of Decoupled Systems-TICT Compounds and Implications Regarding the Development of New Laser Dyes and the Primary Process of Vision and Photosynthesis. *Angew. Chem., Int. Ed.* **1986**, *25*, 971−988.
(47) Letard, J. F.; Lapouyade, R.; Rettig, W. Structure-Photophysics Correlations in a Series of 4-(Dialkylamino)stilbenes: Intramolecular Charge Transfer in the Excited State as Related to the Twist Around the Single Bonds. *J. Am. Chem. Soc.* **1993**, *115*, 2441−2447.
(48) Reichardt, C. Solvatochromic Dyes as Solvent Polarity Indicators. *Chem. Rev.* **1994**, *94*, 2319−2358.
(49) Grabowski, Z. R.; Rotkiewicz, K.; Rettig, W. Structural Changes Accompanying Intramolecular Electron Transfer: Focus on Twisted Intramolecular Charge-Transfer States and Structures. *Chem. Rev.* **2003**, *103*, 3899−4032.
(50) Chiang, C. L.; Tseng, S. M.; Chen, C. T.; Hsu, C. P.; Shu, C. F. Influence of Molecular Dipoles on the Photoluminescence and Electroluminescence of Dipolar Spirobifluorenes. *Adv. Funct. Mater.* **2008**, *18*, 248−257.
(51) Nakabayashi, T.; Wahadoszamen, M.; Ohta, N. External Electric Field Effects on State Energy and Photoexcitation Dynamics of Diphenylpolyenes. *J. Am. Chem. Soc.* **2005**, *127*, 7041−7052.
(52) Chen, B.; Nie, H.; Lu, P.; Zhou, J.; Qin, A.; Qiu, H.; Zhao, Z.; Tang, B. Z. Conjugation versus Rotation: Good Conjugation Weakens the Aggregation-Induced Emission Effect of Siloles. *Chem. Commun.* **2014**, *50*, 4500−4503.
(53) Wu, Q.; Peng, Q.; Niu, Y.; Gao, X.; Shuai, Z. Theoretical Insights into the Aggregation-Induced Emission by Hydrogen Bonding: A QM/MM Study. *J. Phys. Chem. A* **2012**, *116*, 3881−3888.
(54) Yin, S.; Peng, Q.; Shuai, Z.; Fang, W.; Wang, Y.-H.; Luo, Y. Aggregation-Enhanced Luminescence and Vibronic Coupling of Silole Molecules from First Principles. *Phys. Rev. B* **2006**, *73*, 205409.
(55) Al-Attar, H. A.; Griffiths, G. C.; Moore, T. N.; Tavasli, M.; Fox, M. A.; Bryce, M. R.; Monkman, A. P. Highly Efficient, Solution-Processed, Single-Layer, Electrophosphorescent Diodes and the Effect of Molecular Dipole Moment. *Adv. Funct. Mater.* **2011**, *21*, 2376−2382.
(56) Zhao, Z.; Chen, S.; Deng, C.; Lam, J. W. Y.; Chan, C. Y. K.; Lu, P.; Wang, Z.; Hu, B.; Chen, X.; Kwok, H. S.; Ma, Y.; Qiu, H.; Tang, B. Z. Construction of Efficient Solid Emitters with Conventional and AIE Luminogens for Blue Organic Light-Emitting Diodes. *J. Mater. Chem.* **2011**, *21*, 10949−10956.
(57) Gao, Z.; Lee, C. S.; Bello, I.; Lee, S. T.; Chen, R.-M.; Luh, T.-Y.; Shi, J.; Tang, C. W. Bright-Blue Electroluminescence from a Silyl-Substituted Ter-(phenylene−vinylene) Derivative. *Appl. Phys. Lett.* **1999**, *74*, 865−867.
(58) Zhao, Z.; Lam, J. W. Y.; Chan, C. Y. K.; Chen, S.; Liu, J.; Lu, P.; Rodriguez, M.; Maldonado, J.-L.; Ramos-Ortiz, G.; Sung, H. H. Y.; Williams, I. D.; Su, H.; Wong, K. S.; Ma, Y.; Kwok, H. S.; Qiu, H.; Tang, B. Z. Stereoselective Synthesis, Efficient Light Emission, and High Bipolar Charge Mobility of Chiasmatic Luminogens. *Adv. Mater.* **2011**, *23*, 5430−5435.